© 2019. Published by The Company of Biologists Ltd | Development (2019) 146, dev174763. doi:10.1242/dev.174763

RESEARCH ARTICLE

Scribble and Discs Large mediate tricellular junction formation

Zohreh Sharifkhodaei*, Mary M. Gilbert and Vanessa J. Auld‡

ABSTRACT

Junctional complexes that mediate cell adhesion are key to epithelial integrity, cell division and permeability barrier formation. In *Drosophila*, the scaffolding proteins Scribble (Scrib) and Discs Large (Dlg) are key regulators of epithelial polarity, proliferation, assembly of junctions and protein trafficking. We found that Scrib and Dlg are necessary for the formation of the tricellular junction (TCJ), a unique junction that forms in epithelia at the point of convergence of three neighboring cells. Scrib and Dlg are in close proximity with the TCJ proteins Gliotactin (Gli) and Bark Beetle (Bark), and both are required for TCJ protein recruitment. Loss of Bark or Gli led to basolateral spread of the TCJ complex at the cell corners. Loss of the septate junction proteins Nrx-IV and the Na^+/K^+ ATPase also resulted in basolateral spread of the entire TCJ complex at the cell corners. The Scrib PDZ1-2 domains and the Dlg GUK domain are necessary for Bark and Gli localization to the TCJ. Overall, we propose a model in which Scrib and Dlg are key components of the TCJ, and form a complex with Bark and Gli.

KEY WORDS: Scribble, Bark Beetle, Gliotactin, Tricellular junction, Discs Large, *Drosophila*

INTRODUCTION

Permeability barriers are crucial to prevent solute flow across epithelia and other barrier tissues, and are formed by tight junctions in vertebrates and septate junctions (SJs) in invertebrates (Tsukita et al., 2001). Another key junction, the tricellular junction (TCJ), is formed at the corners of epithelial cells at the point of convergence of three tight junctions or SJs. In *Drosophila*, the TCJ is created by a complex of three SJs and a regularly spaced series of plugs or diaphragms that fill the gap at the corners of cells to create the permeability barrier at the corners (Fristrom, 1982; Noirot-Timothée et al., 1982). SJs consist of a ladder-like array below the adherens junctions in epithelial cells (Tepass and Hartenstein, 1994; Tsukita et al., 2001). At the TCJ, the SJs turn 90° and run parallel to the cell corner and are tightly linked to the plugs that line the TCJ (Fristrom, 1982; Noirot-Timothée et al., 1982). SJs are large protein complexes with core components that include Neurexin IV (Nrx-IV) (Baumgartner et al., 1996), Coracle (Cora) (Fehon et al., 1994), the Na^+/K^+ ATPase [the alpha subunit (ATPα) and the β subunit, Nervana 2 (Nrv2)] and Neuroglian (Nrg) (Genova and Fehon, 2003; Paul et al., 2003). Two core transmembrane proteins of the *Drosophila* TCJ have been identified. Gliotactin (Gli), a choline esterase-like protein and a member of the Neuroligin family, is essential for TCJ formation and maturation of the neighboring SJ (Schulte et al., 2003). Bark Beetle (Bark) (also known as Aka, Anakonda) (Byri et al., 2015; Hildebrandt et al., 2015), is a transmembrane protein with a large extracellular triple-repeat domain that is proposed to form the tricellular plug (Byri et al., 2015). Loss of Bark results in barrier defects, disruption of the TCJ and loss of Gli from the TCJ. Loss of Gli does not disrupt the targeting of Bark to the TCJ, supporting a role for Bark in targeting of Gli to the TCJ (Byri et al., 2015). However, how Bark and Gli interact and how these proteins are recruited to the TCJ is not known. Similarly, how the TCJ complex interfaces with the three SJs that converge at the TCJ is not known.

Bark and Gli both have highly conserved PDZ (PSD95, Dlg, ZO1) binding motifs at the C-terminal end suggesting that TCJ formation or function might be mediated by PDZ domain proteins. Gli colocalizes with the PDZ scaffolding protein Discs Large (Dlg; Dlg1) in a range of tissues, including imaginal discs, glia and trachea (Schulte et al., 2003), and forms a protein complex with Dlg (Padash-Barmchi et al., 2013; Schulte et al., 2006). Dlg contains three PDZ domains, an SH3 domain and a GUK domain, but the role of Dlg at the TCJ is not fully understood. Dlg in multiple cellular contexts interacts with another scaffolding protein, Scribble (Scrib), which contains four PDZ domains and a leucine-rich repeat (LRR) domain. Scrib has roles in cell polarity, cell proliferation and trafficking in epithelial cells and scaffolding at the neuromuscular junction (Dow et al., 2007; Humbert et al., 2003; Mathew et al., 2002). The polarity complex containing Scrib and Dlg is crucial for apicobasal polarity establishment by excluding apical proteins from the basolateral surface in epithelial cells (Bilder, 2004; Bilder et al., 2000; Jacob et al., 1987; Woods and Bryant, 1991). Loss of Scrib or Dlg leads to disruption of epithelial organization, loss of polarity, and disc overgrowth. In polarized epithelia, both Scrib and Dlg are localized to the SJ but their role at the TCJ has not been determined. Here, we show that Scrib and Dlg are key components of the TCJ. Scrib and Dlg are in close proximity with the TCJ proteins Gli and Bark, and both scaffolding proteins are key to the integrity of the TCJ.

RESULTS

Scrib is colocalized with Gli and Bark at the TCJ

We hypothesized that there is a scaffolding protein complex at the TCJ, which mediates TCJ formation and function and interacts with Gli and Bark. Gli and Bark both contain conserved PDZ binding motifs. Although these motifs are not necessary for protein localization (Byri et al., 2015; Schulte et al., 2006), we wondered whether the TCJ Gli and Bark proteins interact with PDZ scaffold proteins, such as Scrib and Dlg, and if this interaction facilitates the formation of the TCJ. To test this hypothesis, we first checked the distribution of the TCJ proteins and the scaffolding proteins. We used Bark tagged with GFP (Bark::GFP), a tagged transgene that does not disrupt the PDZ motif, protein function or protein localization to the TCJ (Byri et al., 2015). As expected, both Gli and Bark are restricted to the TCJ within the epithelia of the wing imaginal disc, including the large ribbon-like TCJ of the peripodial epithelia and the smaller TCJ of the columnar epithelia (Fig. 1A-D″). We used a proximity

Department of Zoology, University of British Columbia, Vancouver V6T 1Z4, Canada.
*Present address: Saban Research Institute, Division of Pediatric Gastroenterology, Hepatology, and Nutrition, Children's Hospital Los Angeles, Los Angeles, CA 90027, USA.

‡Author for correspondence (auld@zoology.ubc.ca)

V.J.A., 0000-0003-3976-9186

Received 14 December 2018; Accepted 15 August 2019

Development (2019) 146, dev174763. doi:10.1242/dev.174763

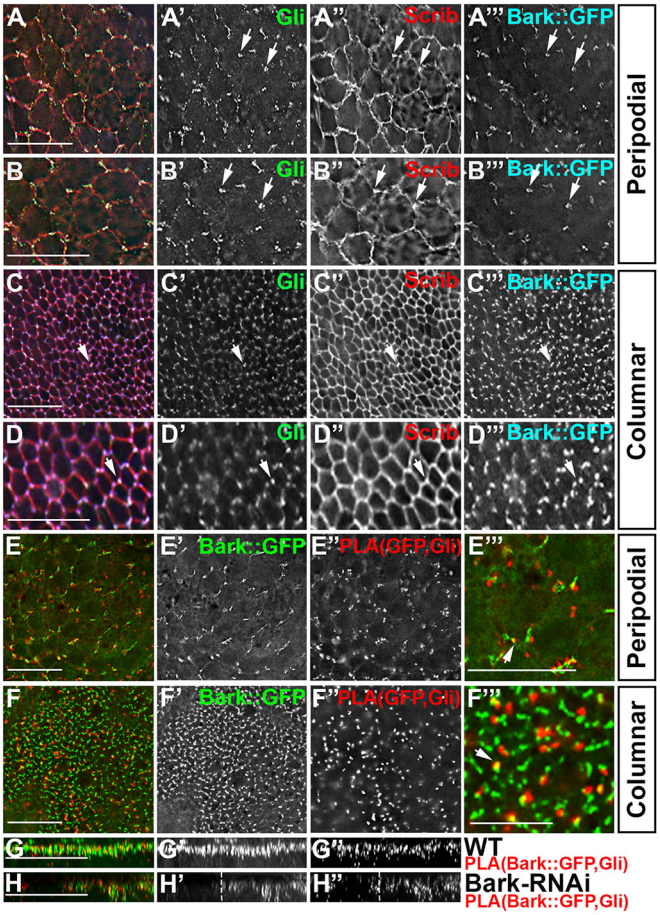

Fig. 1. Scrib is colocalized with Gli and Bark at the TCJ. (A-B‴) Expression pattern of TCJ components in the peripodial epithelia of the wing imaginal disc, immunolabeled for Gli (A′, green in A), Scrib (A″, red in A) and Bark (A‴, blue in A). Scrib was observed all around the cells and it was concentrated at the TCJ with Bark and Gli (arrows). (B-B‴) Digital zoom (1.5×) views of the region shown in A. Gli, Scrib and Bark were colocalized at the TCJ (arrows). (C-D‴) Expression of Gli (C′, green in C), Scrib (C″, red in C), and Bark (C‴, blue in C) at the TCJ in the columnar epithelia of the wing imaginal disc. (D-D‴) Digital zoom (1.5×) views of the region shown in C. Gli, Scrib and Bark were colocalized at the TCJ (arrows). Arrows indicate TCJ with concentrated Scrib. (E-E‴) The PLA between Gli and Bark in the peripodial epithelia with Bark::GFP marking the TCJ (E′, green in E), Bark::GFP+Gli PLA (E″, red in E), and a 2× digital zoom of the merged image (E‴) highlighting Gli and Bark PLA at the peripodial TCJ (arrow). (F-F‴) The PLA between Gli and Bark in the columnar epithelia with Bark::GFP marking the TCJ (F′, green in F), Gli and Bark::GFP PLA (F″, red in F), and a 1.5× digital zoom (F‴) highlighting Gli and Bark PLA at the columnar epithelia TCJ (arrow). (G-G″) Side views for F are shown with Bark::GFP marking the TCJ (G′, green in G), and PLA between Gli and Bark (G″, red in G). (H) Expression of Bark-RNAi led to the reduction of Bark::GFP (H′, green in H) in the apterous (left) side of the wing, and the PLA between Gli and Bark (H″, red in H) was lost compared with the control side (right). All *xy* panels represent a single *z*-slice. Scale bars: 15 µm.

ligation assay (PLA) to confirm that Gli and Bark are in close proximity at the TCJ; PLA can detect proteins in proximities of less than 40 nm (Wang et al., 2015). PLA puncta are generated by annealing of oligonucleotides conjugated to secondary antibodies in close proximity, priming synthesis of a long DNA chain by rolling circle amplification. Therefore, positive PLA puncta can appear diffuse and offset from the origin of the interacting protein pair and associated subcellular structures. We detected Gli+Bark PLA puncta in the peripodial (Fig. 1E‴, arrow) and columnar epithelia (Fig. 1F‴, arrow, and 1G-G″) compared with controls lacking either one of the antibodies (Fig. S1). To further test the specificity of the PLA, we used apterous-GAL4 to drive Bark-RNAi in the dorsal side of the wing imaginal disc. Knockdown of Bark led to loss of the Gli+Bark PLA (Fig. 1H-H″). Thus, our result confirms that Gli and Bark are in close proximity at the TCJ. Using Scrib endogenously tagged with GFP (Scrib::GFP, a homozygous viable insertion) or immunolabeling, we observed that Scrib is localized throughout the bicellular junction and concentrated at the TCJ with Gli and Bark in both the peripodial (Fig. 1A-B‴; arrows) and columnar (Fig. 1C-D‴; arrows) epithelia of the wing imaginal disc. These observations suggest that Scrib, Bark and Gli could form a complex at the TCJ.

Scrib is in close proximity with the TCJ proteins Gli and Bark

To identify how Scrib interacts with the two TCJ proteins Bark and Gli, we used PLA in the wing imaginal disc. We found that Scrib is in close proximity with Gli (Fig. 2A-D″) and Bark (Fig. 2E-H″) in both peripodial (Fig. 2A‴,E‴, arrows) and columnar (Fig. 2B‴,F‴, arrows) epithelia. We noted that the Bark+Scrib PLA puncta appeared to be more extensive within the peripodial cells and extended beyond the TCJ (Fig. 2E‴) into intracellular vesicles, compared with the Gli+Scrib PLA puncta (Fig. 2A‴). We confirmed the specificity of this close proximity using controls lacking either antibody (Fig. S1) and through RNAi-mediated knockdown. Knockdown of Bark using apterous-GAL4 reduced the Bark+Scrib PLA puncta (Fig. 2H-H″). Knockdown of Bark also led to a reduction in the Gli+Scrib PLA puncta (Fig. 2D-D″), which was predicted given that Bark is necessary for recruitment of Gli to the TCJ (Byri et al., 2015). Unexpectedly, knockdown of Gli caused a reduction in the Bark+Scrib PLA puncta (Fig. 2I-I″). With the Gli knockdown, Dlg, Bark and Scrib were still retained at the membrane (Fig. 4E-I″); thus, the reduction of PLA puncta is not due to the loss of the entire TCJ complex from the membrane. These findings suggest that the presence of Bark and Gli is required for the formation of a complex with Scrib at the TCJ and suggest that recruitment of Scrib is dependent on the presence of Gli.

Scrib, Bark and Gli are in close proximity with Dlg at the TCJ

We next wanted to identify whether the PDZ scaffolding protein Dlg is also part of the TCJ complex. Gli has previously been shown to colocalize and form a complex with Dlg at the TCJ (Schulte et al., 2006). Using PLA we determined that Scrib is in close proximity with Dlg throughout the SJ and TCJ domains (Fig. 3A-C″) in both peripodial (Fig. 3A‴, arrow) and columnar (Fig. 3B‴, arrow) epithelia. We confirmed that Gli and Dlg are in close proximity at the TCJ of both peripodial (Fig. 3D‴, arrows) and columnar epithelia (Fig. 3E‴, arrow). We also found that Bark and Dlg are in close proximity at the TCJ (Fig. 3G-I″) of both peripodial (Fig. 3G‴, arrow) and columnar (Fig. 3H‴, arrow) epithelia. We used apterous-GAL4 to knock down Gli in the dorsal side of the wing disc, and observed a reduction in the Bark+Dlg PLA puncta (Fig. 3J-J″) and Gli+Dlg PLA puncta (Fig. 3K-K″). As a control, we also tested for PLA between Gli or Dlg and Talin (Rhea), a component of the focal adhesions at the basal-most side of the columnar epithelia. We used Talin endogenously tagged with mCherry (Talin::mCh), which does not disrupt function or localization (Venken et al., 2011; Klapholz et al., 2015) and we found no Gli+Talin or Dlg+Talin PLA puncta (Fig. S1F-J″).

Quantification revealed that the knockdown of Gli led to a significant reduction in both the Bark+Dlg and Bark+Scrib PLA puncta compared with control (Fig. 3L). Overall, our PLA results suggest that there is a novel TCJ complex between the scaffolding proteins Scrib and Dlg with the membrane proteins Gli and Bark (Table 1). The loss of this complex in the absence of Bark is

Development (2019) 146, dev174763. doi:10.1242/dev.174763

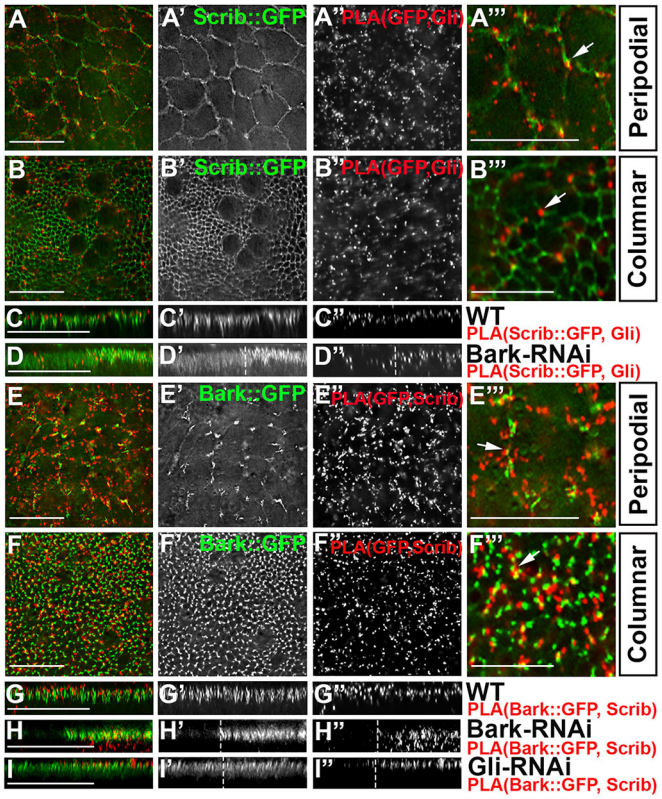

Fig. 2. Scrib is in close proximity with the TCJ proteins Gli and Bark. (A-A‴) The PLA between Scrib and Gli in the peripodial epithelia with Scrib::GFP marking the SJ and TCJ (A′, green in A), PLA between Scrib::GFP+Gli (A″, red in A) and a 2× digital zoom of the region showing PLA concentrated at the TCJ (A‴, arrow). (B-B‴) PLA between Scrib and Gli in the columnar epithelia with Scrib::GFP marking the SJ and TCJ (B′, green in B), PLA between Scrib::GFP+Gli (B″, red in B), and a 1.5× digital zoom of the region showing PLA concentrated at the TCJ (B‴, arrow). (C-C″) Side views for B are shown with Scrib::GFP (C′, green in C) marking the SJ and TCJ level, and PLA between Scrib and Gli (C″, red in C). (D-D″) Expression of Bark-RNAi led to reduction of Scrib::GFP (D′, green in D) in the apterous side (left). The Scrib+Gli PLA (D″, red in D) was reduced in the apterous side compared with the control side (right). (E-E‴) PLA between Scrib and Bark in the peripodial epithelia with Bark::GFP marking the TCJ (E′, green in E), Scrib+Bark::GFP PLA (E″, red in E) and a 2× digital zoom highlighting the PLA clusters (E‴, arrow). (F-F‴) The PLA between Scrib and Bark in the columnar epithelia with Bark::GFP marking the TCJ (F′, green in F), Scrib+Bark::GFP PLA (F″, red in F) and a 1.5× digital zoom highlighting Scrib and Bark PLA concentrated at the TCJ (F‴, arrow). (G-G″) Side views for F are shown with Bark::GFP at the level of the SJ (G′, green in G) and PLA between Scrib and Bark (G″, red in G). (H-H″) Expression of Bark-RNAi led to the downregulation of Bark::GFP (H′, green in H) in the apterous side (left), and the Scrib+Bark PLA (H″, red in H) was reduced compared with the control side (right). (I-I″) Expression of Gli-RNAi. Bark::GFP expression was normal (I′, green in I) but Scrib+Bark PLA was reduced in the apterous side (I″, red in I). All *xy* panels represent a single *z*-slice. Scale bars: 15 µm.

expected given that Bark is necessary to recruit Gli to the TCJ. However, the reduction of the positive PLA between Bark+Dlg and Bark+Scrib in the absence of Gli suggests that the complex requires the presence of Gli to recruit Scrib and Dlg effectively.

Bark and Gli knockdown leads to the basolateral spread of SJ proteins

To test the interactions between Scrib and the other components of the TCJ, we carried out RNAi-mediated knockdown experiments. Bark mutants result in the loss of Gli from the TCJ of the embryonic epidermis or from mutant clones in the wing disc (Byri et al., 2015). RNAi-mediated knockdown of Bark using apterous-GAL4 in the dorsal side of the wing imaginal disc led to a basolateral spread of Scrib (Fig. 4A-D‴) and Dlg (Fig. 4A-B‴), and loss of Gli from the TCJ and cell membrane (Fig. 4A-D‴). Quantification revealed that the basolateral spread was significant for both TCJ and SJ components compared with control (Fig. 4J). Using apterous-GAL4 with Gli-RNAi, we found that Gli downregulation did not disrupt the distribution of Bark at the TCJ (Fig. 4E-E‴) or change the distribution of Scrib (Fig. 4E-E‴) or Dlg (Fig. 4G-G‴) at the TCJ and SJ. However, there was a basolateral spread of Scrib, Dlg and Bark (Fig. 4F-F‴,H-I‴), similar to Nrv2 and Cora (Fig. 4I-I‴). Quantification revealed that the basolateral spread was significant for both TCJ and SJ components compared with control (Fig. 4K). These findings suggest that Bark is necessary for accumulation of Gli at the TCJ, and that loss of both Bark and Gli from the TCJ results in a basolateral spreading of Dlg and Scrib along with other SJ components. This suggests that the presence of both TCJ proteins Bark and Gli are needed to hold the SJ in the normal location just basal to the adherens junction. Given that Bark is present when Gli is knocked down, this also suggests that Gli may play a key role in mediating the interface between the SJ and TCJ.

The TCJ complex is independent of the SJ

Our results suggested a link between the SJ and TCJ domains. To further test the link between the SJ and TCJ, we knocked down the two core SJ components, Nrx-IV and the alpha subunit of the Na/K ATPase pump (ATPα). Using apterous-GAL4, ATPα RNAi-mediated knockdown led to the basolateral spread of Scrib, Gli (Fig. 5A-C‴,M; Fig. S2D-E″) and Bark (Fig. 5D-F‴,M; Fig. S2B-C″). Surprisingly, we found that Scrib, Gli and Bark remained concentrated at the corner of the cells even while the complex spread into more basal regions (Fig. 5C-C‴,F-F‴; Fig. S2C-C″,E-E″), and seemed to reflect an extension of the TCJ complex in the basal direction. Similar to ATPα, we knocked down Nrx-IV or Varicose (Vari, a PDZ domain SJ protein; Bachmann et al., 2008) separately in the dorsal side of the wing imaginal disc. Reduction of Nrx-IV or Vari (data not shown) resulted in the basolateral spread of Scrib, Gli (Fig. 5G-I‴,N; Fig. S2F-G″) and Bark (Fig. 5J-N, Fig. S2H-I″), and again the TCJ protein complex continued to be localized at the cell corners (Fig. 5I-I‴,L-L‴; Fig. S2G-G″,I-I″). Quantification revealed that the TCJ components extended consistently three times the normal length of the TCJ/SJ domain (Fig. 5M,N). Our findings suggest that, even in the absence of SJ components, TCJ proteins are targeted to the corner of the epithelial cells but the tight concentration of the TCJ just under the zona adherens was disrupted and the entire complex extended basally down the cell corners.

Loss of Scrib and Dlg from the SJ does not disrupt the TCJ

To test the interactions between Scrib, Dlg, Gli and Bark at the TCJ, we used RNAi-mediated knockdown of Scrib and Dlg. We regulated the degree of RNAi expression using temperature shifts to 29°C for 24 or 48 h to knock down Scrib to levels that resulted in loss of Scrib from the SJ domain without disrupting epithelial polarity. Loss of Scrib immunolabeling from the entire SJ and TCJ region resulted in loss of Gli (Fig. 6A-C‴) and Bark (Fig. 6D-F‴) from the TCJ. Dlg-RNAi has previously been shown to downregulate Gli at the TCJ (Padash-Barmchi et al., 2013). We then used RNAi to knockdown Dlg to a level that did not interfere with polarity but did remove Dlg immunolabeling from the TCJ and SJ domains. Loss of Dlg from the SJ led to downregulation of Scrib (Fig. 6G-H‴), and loss of Bark (Fig. 6I-K‴) from the TCJ. In attenuating the RNAi, we observed

Development (2019) 146, dev174763. doi:10.1242/dev.174763

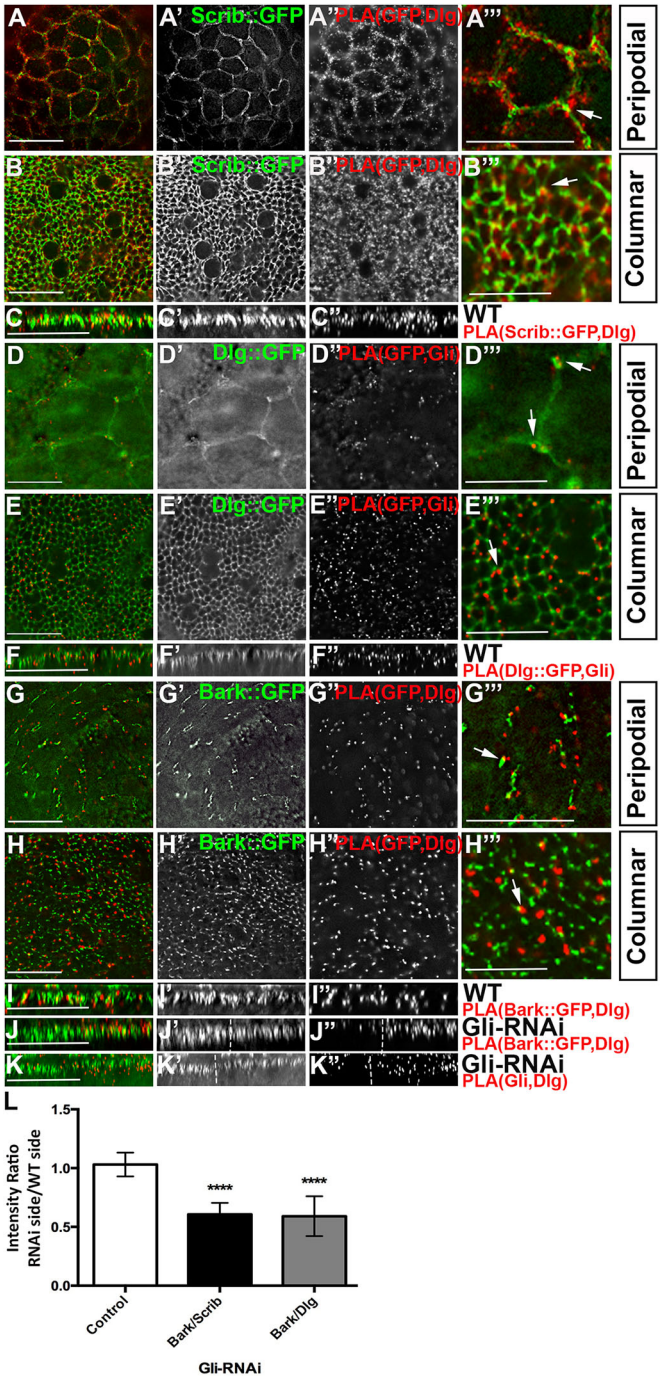

Fig. 3. Scrib and Bark are in close proximity with Dlg at the TCJ. (A-A‴) The PLA between Scrib and Dlg in the peripodial epithelia with Scrib::GFP (A′, green in A), Scrib::GFP+Dlg PLA (A″, red in A) and a 2× digital zoom of the region highlighting the distribution of Scrib::GFP+Dlg PLA around the entire cell perimeter (A‴, arrow). (B-B‴) The Scrib+Dlg PLA in the columnar epithelia with Scrib::GFP (B′, green in B), Scrib::GFP+Dlg PLA (B″, red in B), and a 1.5× digital zoom of the same region highlighting Scrib and Dlg PLA at the level of SJ domain (B‴, arrow). (C-C″) Side views for B with Scrib::GFP (C′, green in C) and the Scrib+Dlg PLA (C″, red in C) at the SJ domain. (D-D‴) The PLA between Gli and Dlg in the peripodial epithelia with Dlg::GFP (D′, green in D), Dlg::GFP+Gli PLA (D″, red in D) and a 2× digital zoom of the region highlighting the distribution of Dlg::GFP+Gli PLA at the TCJ (D‴, arrows). (E-E‴) The PLA between Gli and Dlg in the columnar epithelia with Dlg::GFP (E′, green in E), Dlg::GFP+Gli PLA (E″, red in E), and a 1.5× digital zoom of the same region highlighting Gli and Dlg PLA at the TCJ (E‴, arrow). (F-F″) Side views for E with Dlg::GFP (F″, green in F) and Gli+Dlg PLA (F″, red in F) colocalized at the SJ level. (G-G‴) The Bark+Dlg PLA in the peripodial epithelia with Bark::GFP (G′, green in G), Bark::GFP+Dlg PLA (G″, red in G) and a 2× digital zoom of the same region highlighting the Bark+Dlg PLA at the TCJ (G‴, arrow). (H-H‴) The Bark+Dlg PLA in the columnar epithelia with Bark::GFP (H′, green in H), Bark::GFP+Dlg PLA (H″, red in H), and a 1.5× digital zoom of the region highlighting the Bark+Dlg PLA at the TCJ (H‴, arrow). (I-I″) Side projections for H with Bark::GFP (I′, green in I) and Bark+Dlg PLA (I″, red in I). (J-K″) Expression of Gli-RNAi in the left side of the wing. Whereas Bark::GFP (J′,K′, green in J,K) is expressed through the SJ, the Bark::GFP+Dlg PLA (J″, red in J), and Gli+Dlg PLA (K″, red in K) was reduced on the dorsal side. (L) Statistical analysis of the PLA intensity ratio in Gli-RNAi on the apterous side normalized to that of the control non-apterous side. The degree of PLA signal between Bark::GFP and Scrib, and Bark::GFP and Dlg was significantly reduced compared with apterous-GAL4 line alone (n=13 discs, ****P<0.0001, mean±s.d., one-way ANOVA). All image xy panels represent a single z-slice. Scale bars: 15 µm.

examples in which Dlg and Scrib were lost from the SJ but still retained at the TCJ in patches of cells (Fig. 6C-C‴, arrows). In these instances, when Scrib or Dlg were still concentrated at the TCJ (but not the SJ domain), Gli, Bark and Dlg or Scrib were also retained (Fig. 6C-C‴,F-F‴,K-K‴, arrows). These results suggest that the formation of the TCJ protein complex is dependent of the presence of both Dlg and Scrib at the cell corners and point to a key role for both Dlg and Scrib in mediating the recruitment of Bark and Gli to the TCJ.

To identify the role of Scrib and Dlg in the control of SJs, we assayed the SJ protein Nrv2, the beta subunit of the Na/K ATPase, and a core component of the SJ (Genova and Fehon, 2003; Paul et al., 2003). Loss of Scrib and Dlg caused the reduction and basolateral spread of Nrv2 (Fig. 7). The expression and localization of the adherens junction protein E-cad (Shotgun) was unaffected (Fig. 7A‴,B‴,D‴,E‴). With attenuated Scrib or Dlg knockdown, as before, Scrib or Dlg were retained at the TCJ (and immunolabeling lost from the SJ). In these regions, Nrv2 was still localized to the SJ domain around the columnar epithelia (Fig. 7C″,F″, arrows). Even with the variability of the RNAi-mediated knockdown, our results suggest that the presence of Scrib and Dlg at the TCJ is required for the correct localization of the SJ complex just below (basal to) the adherens junction.

Scrib PDZ1-2 domains are essential for Scrib interactions at the TCJ

Scrib and Dlg contain a range of conserved protein domains known to scaffold protein complexes. Scrib contains a series of LRR domains in the N-terminal half of the protein and four PDZ domains in the C-terminal half (Bilder and Perrimon, 2000) (Fig. 8G). To determine which domains of Scrib might be important for control of the TCJ complex, we utilized previously characterized *scrib* alleles that lack one or more of the PDZ domains (Zeitler et al., 2004). We tested the *scrib[dt6]* mutant, which retains the LRR domains but lacks all four PDZ domains, and the *scrib[dt12]* mutant, which lacks the third and fourth PDZ domains and retains the first and second PDZ domains (Fig. 8G) (Zeitler et al., 2004). Both mutants, when placed over the *scrib[673]* null allele, generate wing discs with different degrees of epithelial disruption (Zeitler et al., 2004). In the *scrib[dt6]/scrib[673]* discs, the distribution of the TCJ protein complex, including Dlg, Gli (Fig. 8A-C‴) and Bark (Fig. 8A,A″), was disrupted along with the AJ protein E-cad (Fig. 8B-C‴). However, in the *scrib[dt12]/scrib[673]* discs, Dlg and Gli (Fig. 8D-F‴) were correctly localized at the TCJ and Mcr, an SJ protein, localized normally (Fig. 8E-E‴). However, Bark (Fig. 8D,D″) was localized to both the bicellular SJ and the TCJ in the *scrib[dt12]/scrib[673]* discs. Loss of the Scrib PDZ2 domain leads to a cytoplasmic distribution suggesting that PDZ2 is required

Development (2019) 146, dev174763. doi:10.1242/dev.174763

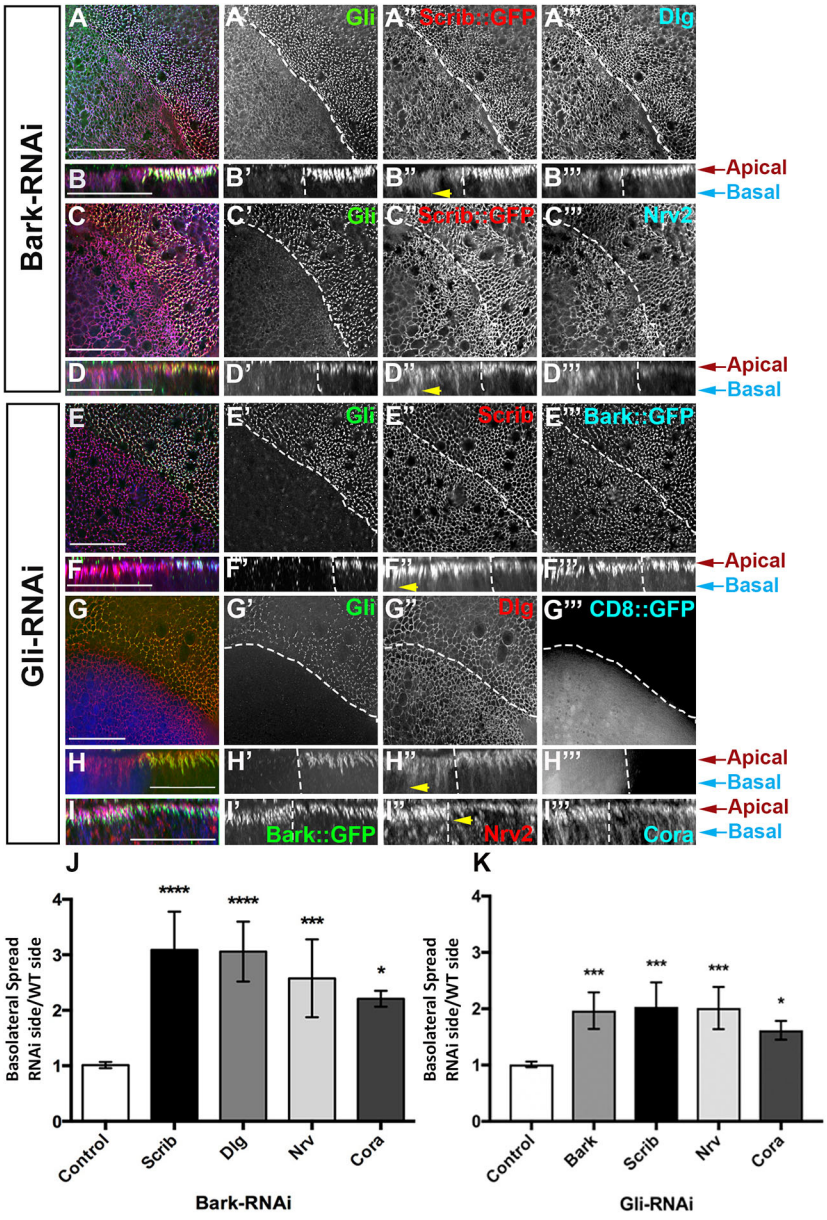

Fig. 4. Bark and Gli knockdowns lead to the basolateral spread of SJ proteins. (A-D‴) Expression of Bark-RNAi led to the reduction of Gli (A′,C′, green in A,C) and basolateral spread of Scrib (A″,C″, red in A,C), Dlg (A‴, blue in A) and Nrv2 (C‴, blue in C). (B-B‴,D-D‴) Side projections for A and C are shown below. Arrowheads in B″ and D″ show the basolateral spread of Scrib::GFP. (E-I‴) Expression of Gli-RNAi (E′, green in E) led to basolateral spread of Scrib (E″, red in E) and Bark (E‴, blue in E) along with Dlg (G″,H″, red in G,H). mCD8::GFP marked the dorsal side (left) (G‴,H‴, blue in G,H). Side projections for each panel are shown below (F-F‴,H-H‴). Arrowheads indicate the basolateral spread of Scrib (F″) and Dlg (H″). (I-I‴) Side projection views indicating the basolateral spread of Bark (I′, green in I), Nrv2 (I″, red in I) and Cora (I‴, blue in I). Arrowhead indicates the extent of basolateral spread. (J,K) Statistical analysis of basolateral spread of junctional proteins on the dorsal side normalized to that of the control ventral side. The degree of Scrib, Nrv2, Cora and Bark basolateral spread was significant compared with apterous-GAL4 line alone in Bark-RNAi and Gli-RNAi (n=5 discs, ****P<0.0001, ***P<0.001, *P<0.05, mean±s.d., one-way ANOVA). All *xy* panels represent a single *z*-slice. In image panels, dashed lines indicate the apterous expression boundary. Scale bars: 15 µm.

for Scrib recruitment to the lateral membrane and SJs (Albertson et al., 2004). The *scrib[dt6]* mutant protein is localized along the basolateral membrane and lacks polarization in wing epithelia, whereas the *scrib[dt12]* protein lacking the PDZ3-4 domains is concentrated at the SJ (Zeitler et al., 2004). Our findings suggest that the PDZ1-2 domains are essential for polarity, and that the disruption of the SJ and TCJ complex formation is likely due to a disruption in polarity or a failure to recruit Scrib to the SJ domain. Our results also point to a differential role of the PDZ3-4 domains in the recruitment of Bark compared with Gli.

Table 1. Summary of TCJ protein PLA interactions in control and apterous-GAL4 driven RNAi for Bark and Gli

		PLA combinations and effects		
		+Gli	+Dlg	+Scrib
Control	Bark	At TCJ (Fig. 1)	At TCJ (Fig. 3)	At TCJ (Fig. 2)
	Gli		At TCJ (Fig. 3)	At TCJ (Fig. 2)
	Dlg	At TCJ (Fig. 3)		At TCJ and SJ (Fig. 3)
Bark-RNAi	Bark	Absent (Fig. 1)	ND	Reduced (Fig. 2)
	Gli		ND	Reduced (Fig. 2)
Gli-RNAi	Bark	ND	Reduced (Fig. 3)	Reduced (Fig. 2)
	Gli		Reduced (Fig. 3)	ND

Each PLA combination is indicated with: Bark – Bark::GFP; Scrib – Scrib::GFP or anti-Scrib antibody; Dlg – Dlg::GFP or anti-Dlg antibody; Gli – anti-Gli antibody. ND, not determined.
The figure corresponding to each of the PLA combinations and effects is indicated.

Development (2019) 146, dev174763. doi:10.1242/dev.174763

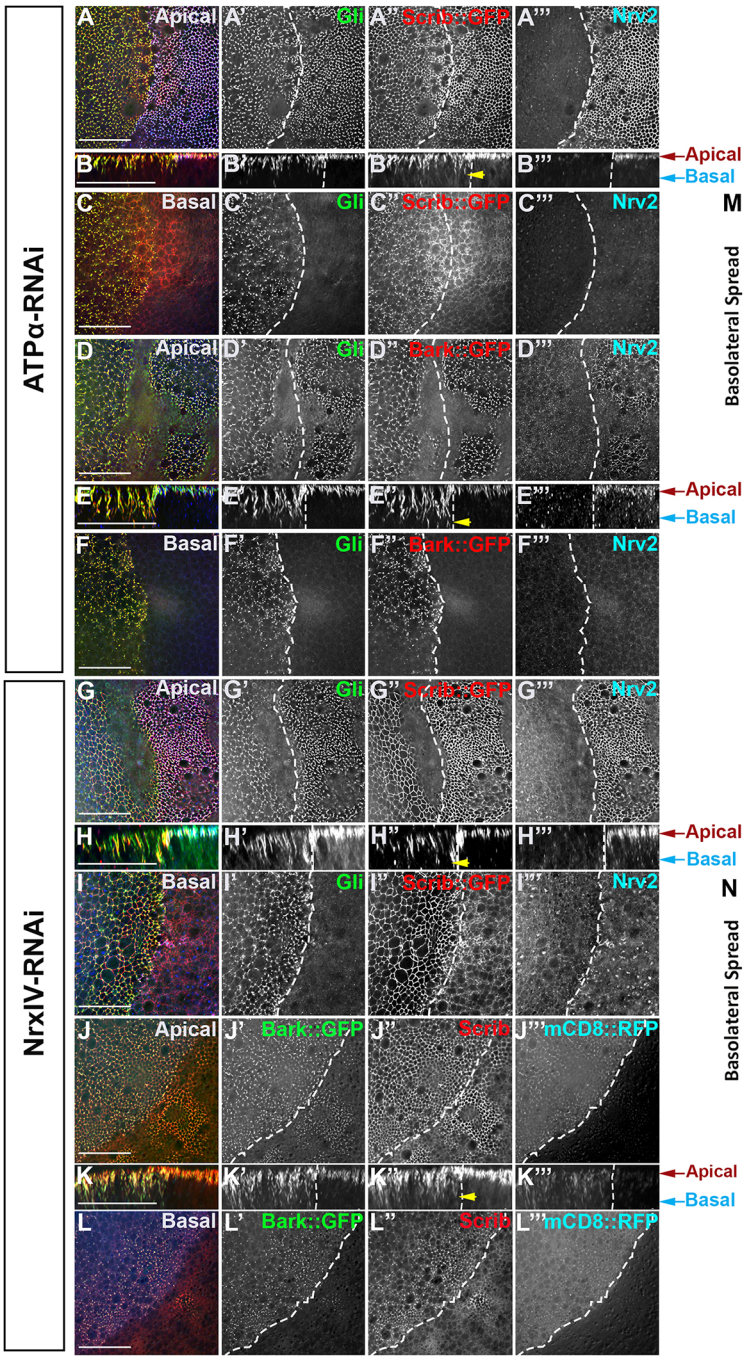

Fig. 5. TCJ formation is independent of the SJ. (A-F‴) ATPα-RNAi-mediated knockdown in the apterous side (left) led to the basolateral spread of Gli (A′,D′, green in A,D), Scrib (A″, red in A) and Bark (D″, red in D) and downregulation of the SJ protein Nrv2 (A‴,D‴, blue in A,D). (B-B‴,E-E‴) Side projections for A and D, highlighting the basolateral spread (arrows). (C-C‴,F-F‴) Gli (C′,F′, green in C,F), Bark (F″, red in F) and Scrib (C″, red in C) were concentrated to the TCJ at the level of the SJ domain [apical; Z slice=9 (A) and Z slice=16 (D)] and still remained in the TCJ in more basal regions [basal; Z=24 (C) and Z=56 (F)], away from the SJ. (G-L‴) Nrx-IV-RNAi-mediated knockdown led to downregulation of Nrv2 (G‴, blue in G) and basolateral spread of Gli (G′, green in G), Scrib (G″,J″, red in G,J) and Bark (J′, red in J). (H-H‴,K-K‴) Side projections for G and J, highlighting the basolateral spread (arrows). (I,L) Gli (I′, green in I), Scrib (I″,L″, red in I,L) and Bark (L′) were concentrated at the corner of the cells basally [basal; Z=50 (I) and Z=41(L)], away from the SJ [apical; Z=34 (G) and Z=26 (J)]. mCD8::RFP (J‴,L‴, blue in J,L) marked the apterous side (left) where Nrx-IV-RNAi is expressed. (M,N) Statistical analysis of the basolateral spread of junctional proteins on the dorsal side normalized to that of the control ventral side. The degree of basolateral spread of Scrib, Gli and Bark are each significant compared with the control in ATPα-RNAi (M) and Nrx-IV-RNAi (N). (n=6 discs, ****P<0.0001, mean±s.d., one-way ANOVA). All *xy* panels represent a single *z*-slice. In image panels, dashed lines indicate the apterous expression boundary. Scale bars: 15 µm.

The Dlg GUK domain is required for TCJ protein localization and Bark trafficking

Dlg is also a scaffolding protein and contains three PDZ, a Src homology 3 (SH3), and guanylate kinase (GUK) domain (Fig. 9H) (Woods and Bryant, 1991). Loss or disruption of the PDZ domains leads to a complete disruption of epithelia polarity (Hough et al., 1997; Woods and Bryant, 1991) and thus it was not possible to assess SJs in wing discs of these mutants. Both the SH3 and GUK domains can interact with other protein complexes and the interaction between the SH3 and GUK domains regulates the accessibility of the GUK domain to binding with other proteins (Newman and Prehoda, 2009; Shin et al., 2000). To investigate the role of the Dlg domains, we used two *dlg1* mutants. *dlg1[12]* (also known as *dlg1[m30]*) changes a highly conserved Leu to Pro in the SH3 domain (Tejedor et al., 1997). *dlg1[6]* (also known as *dlg1[v59]*) lacks the last two-thirds of the GUK domain (Woods and Bryant, 1991). Both mutant proteins are stable (Mendoza et al., 2003; Woods et al., 1996) and retain function at the neuromuscular junction in terms of clustering of Shaker channels (Tejedor et al., 1997). In the *dlg1[12]* wing discs in both peripodial and columnar epithelia, Gli and Bark were concentrated at the cell membrane, and Dlg was also recruited to the membrane (Fig. 9A-A‴). Gli and Bark were present in those regions where Scrib was concentrated at what appeared to be junctions (Fig. 9A-B‴, arrows); however, it was difficult to detect whether these regions were intact TCJs as polarity was severely disrupted. In the *dlg1[6]* discs, Scrib was recruited to the bicellular junctions at the apical side of the columnar epithelia (Fig. 9D″), and the peripodial epithelia (Fig. 9C″) similar to the

Development (2019) 146, dev174763. doi:10.1242/dev.174763

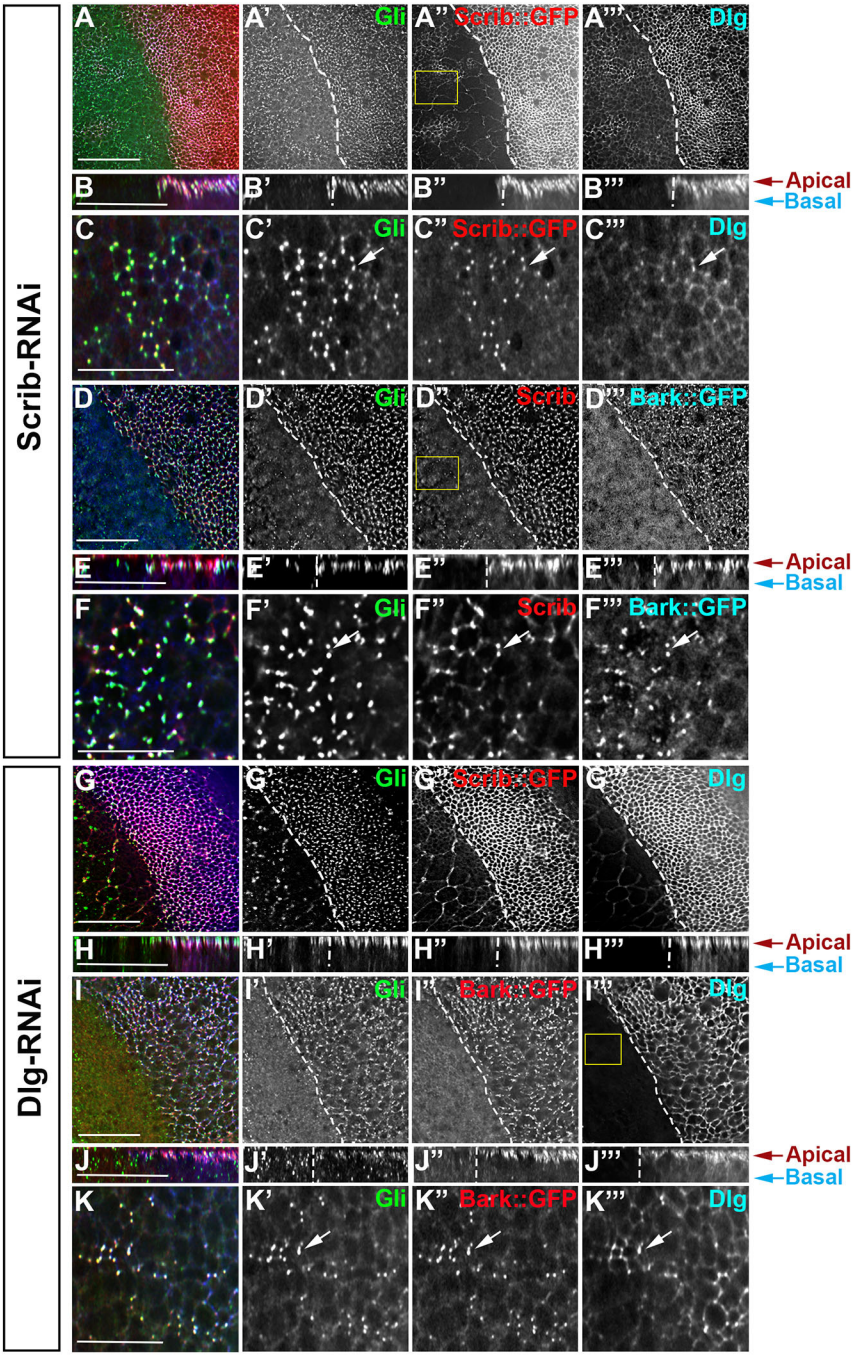

Fig. 6. Loss of Scrib and Dlg from the SJ does not disrupt the TCJ. (A-C‴) Scrib RNAi-mediated knockdown (A″, red in A) led to loss of Gli (A′, green in A) and Dlg (A‴, blue in A) from the SJ. (B-B‴) Side projections for A are shown with apical and basal indicated by arrows. (C-C‴) Digital magnification (1.6×) views of the boxed region in A″. Gli (C′, green in C), Scrib (C″, red in C) and Dlg (C‴, blue in C) were retained in the corner of the cells (arrows). (D-F‴) Scrib RNAi -mediated knockdown (D″, red in D) resulted in loss of Gli (D′, green in D) and Bark (D‴, blue in D). (E-E‴) Side projections for each panel are shown with apical and basal indicated by arrows. (F-F‴) Digital magnification (1.6×) views of the boxed region in D″. Bark was retained at the TCJ (F‴, arrows; blue in F) along with Gli (F′, green in F) and Scrib (F″, red in F). (G-K‴) Dlg RNAi-mediated knockdown (G‴, I‴, blue in G,I) led to the loss of Scrib (G″, red in G), Gli (G′,I′, green in G,I) and Bark (I″, red in I). (K-K‴) Digital zoom (1.4×) of the boxed area in I‴. Bark (K″, arrow; red in K), Gli (K′, arrow; green in K) and Dlg (K‴, arrow; blue in K) were restricted to the corner of the cells. (H-H‴,J-J‴) Side projections for each panel are shown with apical and basal indicated by arrows. All *xy* panels represent a single *z*-slice. Dashed lines indicate the apterous expression boundary. Scale bars: 15 µm.

mutant Dlg protein (Fig. 9C‴, arrow). Scrib was concentrated in the apical domain and not found in more basal regions (Fig. 9E″). Bark was localized throughout the epithelium but not at the membrane and concentrated in intracellular puncta (Fig. 9C-E‴). We used E-cad to define the cell membrane and observed that the Bark puncta corresponded to intracellular vesicles (Fig. 9C-E‴). In the *dlg1[6]* mutant, Gli was not colocalized with Bark and was concentrated in smaller intracellular vesicles (Fig. 9F′,F‴). Gli localization to the TCJ is controlled by endocytosis and lysosome-mediated degradation (Padash-Barmchi et al., 2010) and so we tested for the distribution of Gli and Bark with endosomes. In *dlg1[6]* wing discs, Gli vesicles frequently colocalized with the late endosomal marker, Rab7 (Fig. 9F″,F‴; arrows) but the Bark intracellular vesicles did not (Fig. 9F′,F″). To confirm these observations, we knocked down Dlg (using RNAi) and this also led to the presence of Bark in intracellular vesicles (Fig. 9G′, arrows) that were distinct from the Gli-positive vesicles. Our results suggest that in the absence of Bark and/or Dlg, Gli is not retained at the TCJ, possibly due to increased endocytosis of Gli similar to the effects observed with the loss of the Gli PDZ binding motif (Padash-Barmchi et al., 2013). Overall, our results suggest that it is the collective interactions of Scrib and Dlg that result in the presence of Bark and Gli at the TCJ and that this protein complex requires the Scrib PDZ domains and the presence of the Dlg GUK domain.

DISCUSSION

We have identified a complex at the TCJ of imaginal disc epithelia that consists of Scrib, Dlg and the two TCJ proteins Gli and Bark. Scrib

Development (2019) 146, dev174763. doi:10.1242/dev.174763

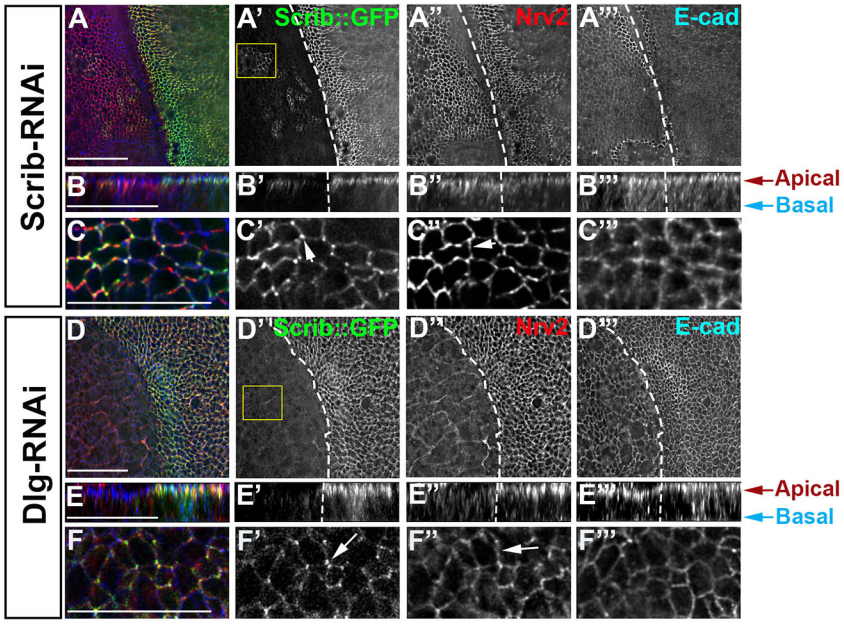

Fig. 7. The presence of Scrib and Dlg are required for SJ localization. (A-C‴) Scrib RNAi-mediated knockdown (A′, green in A) led to basolateral spread of Nrv2 (A″, red in A) whereas E-cad expression was unaffected (A‴, blue in A). (B-B‴) Side projections for A are shown with apical and basal indicated by arrows. (C-C‴) Digital magnification (2.4×) views of the boxed region in A highlighting normal Nrv2 localization to the SJ (C″, arrow; red in C) when Scrib was retained at the TCJ (C′, green in C). (D-F‴) Dlg RNAi-mediated knockdown resulted in downregulation of Scrib (D′, green in D) and Nrv2 (D″, red in D), whereas E-cad expression was normal (D‴, blue in D). (E‴) Side projections for D are shown with apical and basal indicated by arrows. (F-F‴) Digital magnification (2.4×) views of the boxed region in D highlighting normal localization of Nrv2 to the junction (F″, arrow; red in F) when Scrib was retained at the TCJ (F′, arrow; green in F). All *xy* panels represent a single *z*-slice. Dashed lines indicate the apterous expression boundary. Scale bars: 15 µm.

and Dlg are in close proximity with Gli, Bark and Dlg at the TCJ, and loss of any component from the TCJ disrupts the integrity of the complex. Although Bark is crucial for recruitment of Gli to the TCJ, Gli also plays a role in complex formation, as loss of Gli changed the proximity between Bark+Scrib and Bark+Dlg. We found that loss of Scrib and Dlg proteins from the TCJ (but not the SJ) led to the loss of Bark, Gli, and Scrib or Dlg. The last region where Scrib and Dlg were detected before entire loss from the cell membrane was at the TCJ. Only when Scrib or Dlg was lost from the TCJ was the TCJ complex disrupted. This leads us to suggest a model in which the TCJ complex is interdependent whereby all four components (Bark, Gli, Scrib and Dlg) are required for formation of a stable TCJ complex.

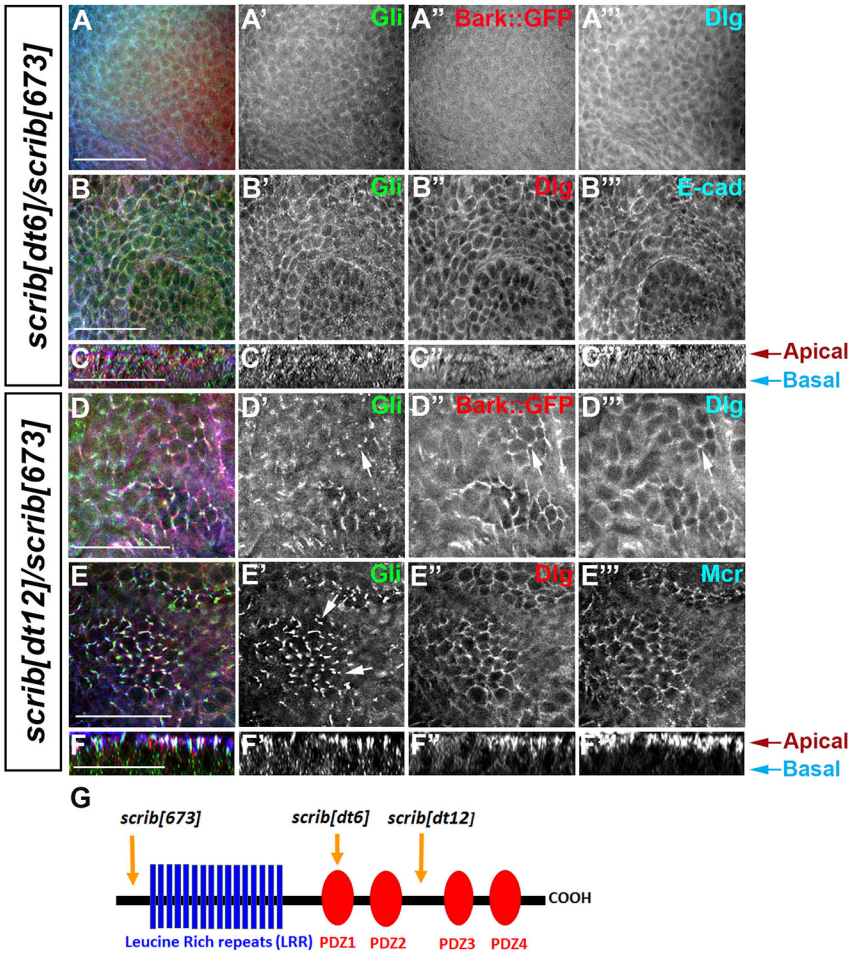

Fig. 8. Scrib PDZ1-2 domains are essential for Scrib interactions at the TCJ. (A-C‴) A *scrib[dt6]*/*scrib[673]* mutant wing imaginal disc. Loss of all four PDZ domains disrupted the localization of Gli (A′,B′, green in A,B), Bark (A″, red in A), Dlg (A‴,B‴; blue in A, red in B) and E-cad (B‴, blue in B) from the TCJ in the columnar epithelia. (C-C‴) Side projections for B are shown with apical and basal indicated by arrows. (D-F‴) A *scrib[dt12]*/*scrib[673]* mutant wing imaginal disc. The presence of the Scrib PDZ1-2 domains retains the normal localization of Gli (D′,E′, arrows; green in D,E) and Bark (D″, arrow; red in D) to the TCJ, Dlg (D‴,E‴; blue in D, red in E) to both TCJ and SJ, and Mcr (E‴, blue in E) to the SJ of the columnar epithelia. (F-F‴) Side projections for E are shown with apical and basal indicated by arrows. All panels represent a single *z*-slice. Scale bars: 15 µm. (G) Scribble (Scrib) protein consists of 16 leucine-rich repeats and four PDZ domains. Arrows indicate the location of premature stop codon in *scrib[673]*, *scrib[dt6]* and *scrib[dt12]*.

Development (2019) 146, dev174763. doi:10.1242/dev.174763

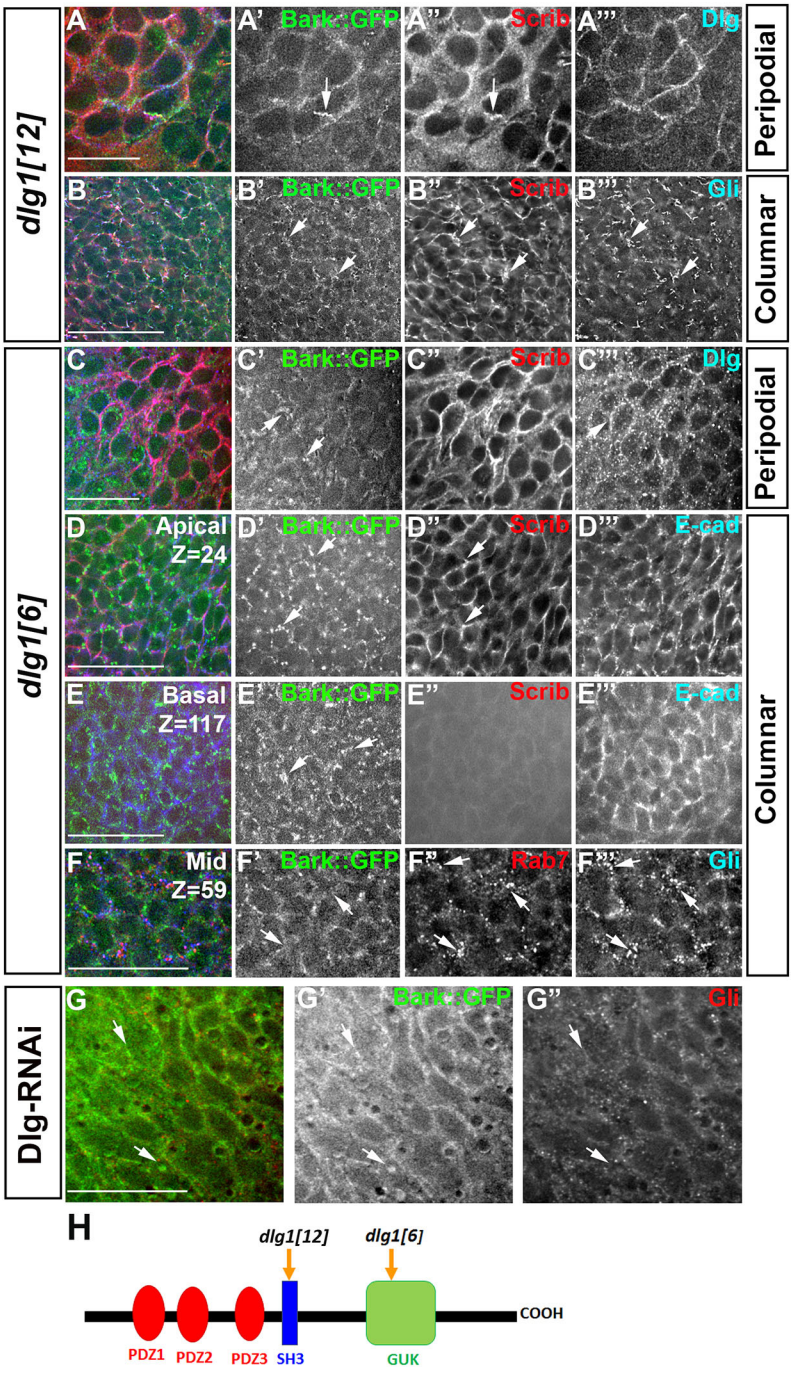

Fig. 9. The Dlg GUK domain is required for TCJ protein localization. (A-B‴) A mutant *dlg[12]* wing imaginal disc showing the peripodial (A-A‴) and columnar (B-B‴) epithelia. Mutant Dlg is mislocalized in peripodial cells (A‴, blue in A), but Bark (A′,B′, green in A,B) and Gli (B‴, blue in B) were present when Scrib (A″, B″, red in A,B) was recruited and concentrated in the plasma membrane (arrows). (C-F‴) A mutant *dlg[6]* wing imaginal disc showing the peripodial (C-C‴) and columnar (D-F‴) epithelia. Mutant Dlg protein is mislocalized (arrow) in peripodial cells (C‴, blue in C) and led to the disruption of Bark trafficking (C′, arrows). Bark was retained in large intracellular vesicles that were spread throughout the columnar epithelia (D′,E′, arrows; green in D,E). Scrib (D″, arrows; red in D) was frequently recruited to bicellular junctions and was apically localized. Owing to loss of polarity, E-cad was localized at the membrane from apical (D‴, blue in D) to more basal levels (E‴, blue in E). (F) The Bark vesicles (F′, arrows; green in F) were not colocalized with Rab7 (F″, red in F) whereas Gli vesicles (F‴, blue in F) frequently colocalized with Rab7 (arrows). (G-G‴) Dlg RNAi-mediated knockdown also showed Bark was concentrated in large intracellular vesicles (G′, arrows; green in G) that were not positive for Gli (G″, arrows; red in G). All panels represent a single *z*-slice. Scale bars: 15 µm. (H) The Discs Large (Dlg) protein includes three PDZ domains, one Src homology 3 (SH3) domain and a guanylate kinase (GUK) domain. Arrows show the locations of the *dlg[12]* and *dlg[6]* mutations.

The TCJ complex also regulates the organization of the bicellular SJs. Knockdown of both TCJ proteins Gli and Bark results in the basolateral spread of Scrib, Dlg, and other SJ components, and knockdown of ATPα and Nrx-IV, two main SJ proteins, leads to the spread of Gli, Bark and Scrib at the TCJ. This supports prior work where the loss of Gli and Dlg in embryonic epithelia leads to the basolateral spread and mislocalization of the SJ components within the membrane (Oshima and Fehon, 2011; Schulte et al., 2006). In our model, we propose that Gli is key to linking the SJ with the TCJ as loss of Gli does not affect the recruitment of Bark to the cell corners yet leads to the spread of the SJ proteins. Our results suggest that the formation of the Scrib/Dlg/Gli/Bark complex at the cell corners is independent of the presence of the SJ. However, there is a strong relationship between the SJ and TCJ as the tight localization of each of these junctions just basal to the zona adherens requires the presence of the other. These results mirror previously suggested models of the TCJ based on scanning and transmission electron microscopic analyses (Noirot-Timothée et al., 1982; Fristrom, 1982), in which the distribution and periodicity of the plugs of the TCJ are matched with the descending SJ strands, suggesting an intimate association of both junctional complexes.

Scrib, in partnership with Dlg, has been found to be key to complex formation in multiple tissues. Scrib and Dlg are components of the Scrib polarity complex in polarized epithelia. Dlg is required to stabilize the Scrib association with the membrane and Scrib is essential to recruit Lethal giant larvae [Lgl (l(2)gl] to the cortical

Development (2019) 146, dev174763. doi:10.1242/dev.174763

domain (Bilder et al., 2000). Scrib forms a complex with Dlg at the neuromuscular junction, where the Dlg GUK domain binds the GUK-holder protein, which in turn binds to the Scrib PDZ2 domain (Albertson et al., 2004; Albertson and Doe, 2003; Mathew et al., 2002). In vertebrate epithelia, Scrib is a regulator of tight junction function; knockdown of Scrib disrupts the epithelial barrier and inhibits tight junction reassembly leading to discontinuous patterns of ZO-1 (Tjp1) and occludin at cell-cell contacts (Ivanov et al., 2010). Thus, Scrib is important for tight junction assembly and can partner with other proteins to control junctional integrity. However, the role of Scrib at the tricellular tight junction and its interaction with the vertebrate TCJ proteins tricellulin (Marveld2) or lipolysis-stimulated lipoprotein receptor (LSR) has not been tested.

Both Scrib and Dlg contain protein-binding domains known to scaffold a wide range of proteins. In our study, we found that the PDZ domains of Scrib plus the GUK domain of Dlg play an important role in the formation of the TCJ. In *scrib* mutants lacking the PDZ domains, apical proteins and adherens junction markers can form, albeit in the context of disorganized epithelial structure (Zeitler et al., 2004). We found that loss of all four Scrib PDZ domains (*scrib[dt6]*) disrupts Gli, Bark and Dlg distribution whereas in a *scrib* allele retaining the first and second PDZ domains (*scrib[dt12]*), Gli and Dlg proteins are localized to the TCJ. This mirrors current work showing that Dlg localization is reduced in *scrib[dt6]* somatic clones, leading to the suggestion that Dlg localization requires the presence of the first and second PDZ domain of Scrib (Nakajima et al., 2019). Of note is the localization of Bark throughout the bicellular and TCJ domain in the *scrib[dt12]* allele, suggesting a further role for the PDZ3-4 domains in the specific localization to the TCJ. For Dlg, we determined that the GUK domain is important in formation of the TCJ. The SH3 and GUK domains interact with a range of binding proteins including an intramolecular SH3-GUK association. Mutations in SH3-GUK interaction disrupt protein complex assembly (McGee and Bredt, 1999; Nix et al., 2000), and dysregulate the binding of proteins to the GUK domain (Qian and Prehoda, 2006). However, SH3-GUK intramolecular interaction is not required for the localization of Scrib and Dlg to the SJ (Newman and Prehoda, 2009). Similar to the previous studies, we found that in *dlg[12]*, which interferes with the SH3 and GUK interaction, Dlg and Scrib are localized to the membrane. However, Gli and Bark are mislocalized through the bicellular SJ, possibly due to the dysregulation of complex assembly at the TCJ. Our results suggest that Scrib PDZ1-2 and the Dlg GUK domains are essential for recruitment of the TCJ protein complex; however, it is unknown whether the interaction with Dlg and the two TCJ membrane proteins is direct or indirect through intermediary proteins.

In summary, we have determined that the scaffolding proteins Scrib and Dlg play an important role in TCJ formation, in recruiting Bark and Gli to the junction, and that this complex is mutually dependent for stability at the corners of polarized epithelia. At the TCJ, the three converging SJs turn 90° to run parallel to the TCJ, where both complexes form extensive and stereotypic contacts (Fristrom, 1982; Noirot-Timothée et al., 1982). We propose that the TCJ complex and the SJ complex are linked at the corners likely through the actions of Gli and that each complex is mutually dependent to ensure the tight localization of both just basal to the AJ.

MATERIALS AND METHODS

Fly stocks

The following fly strains were used: *Bark[L200]*, *Bark::GFP* or *Df(2L)Excel6009*, *Bark::GFP* (Byri et al., 2015), *scrib[dt6]*, *scrib[dt12]*, *scrib[673]* (Zeitler et al., 2004). UAS-Scrib-RNAi (v105412), UAS-Dlg-RNAi (v41134), UAS-Bark-RNAi (v52608), UAS-NrxIV-RNAi (v8353) and UAS-ATPα-RNAi (v12330) were from the Vienna *Drosophila* Resource Center (VDRC). UAS-Gli-RNAi (NIG3903R-3) and *dlg1[6]* (DGRC106785) were from the Kyoto *Drosophila* Stock Center. UAS-Gli-RNAi (Bl:31869), *dlg1[12]* (Voelker et al., 1985), Scrib::GFP, Dlg::GFP (Morin et al., 2001), Talin::mCh (Venken et al., 2011) and apterous-GAL4 were from the Bloomington *Drosophila* Stock Center.

Titrating the degree of Scrib and Dlg knockdown

We used apterous-GAL4 drivers to express an RNAi line known to effectively knock down Scrib or Dlg. To regulate the degree of Scrib knockdown, the ap-GAL4; Scrib-RNAi larvae were moved from 25°C to 29°C for 24-48 h. This temperature shift resulted in loss of Scrib from the SJ without disrupting epithelial polarity. For Dlg knockdown, we used Dlg RNAi (VDRC v41134) without Dicer-2 at 25°C as previously described (Padash-Barmchi et al., 2013). Discs were assessed that had lost SJ localization but retained patches of Scrib or Dlg at the TCJ.

Statistical analysis

All statistical tests were calculated and presented graphically with GraphPad Prism 6. Immunofluorescence levels and distance spread were quantified using ImageJ (Schneider et al., 2012). For controls, apterous-GAL4 alone was used. The fluorescence intensity was measured and calculated in a single *z*-slice at the plane of the SJ domain. The mean intensity was calculated using the same fixed-size square in two areas: the apterous side (RNAi) versus the non-apterous side (WT) (Fig. 3). For each box, the mean intensity was calculated using ImageJ and the ratio of apterous/non-apterous calculated. The length of the basolateral spread was measured for the apterous side (RNAi) compared with the non-apterous side (WT) using side projections. Side projections were obtained using Softworx and a width of one cell diameter. Using ImageJ, the lower limit for each immunolabeled protein was determined (Figs 4, 5, arrows), a line drawn and the distance to the top of the SJ domain measured. The distance spread was calculated as a ratio (RNAi side over non-apterous side). For all ratios, the significance was determined using one-way ANOVA with Tukey's post-hoc test. For all statistics, the mean plus standard deviation is indicated.

Immunolabeling

Third instar larval imaginal discs were immunolabeled as described previously (Schulte et al., 2006). Primary antibodies were: mouse anti-Gli 1F6.3 at 1:200 (Auld et al., 1995), rabbit anti-Gli at 1:300 (Venema et al., 2004), mouse anti-Dlg 4F3 at 1:200 (Developmental Studies Hybridoma Bank) (Parnas et al., 2001), rat anti-DE-Cadherin at 1:50 (Developmental Studies Hybridoma Bank) (Oda et al., 1994), guinea pig anti-Mcr at 1:800 (Hall et al., 2014), rabbit anti-Scrib at 1:2500 (Albertson and Doe, 2003), rabbit anti-Nrv2.1 at 1:1000 (Sigma-Aldrich, SAB2700166), rabbit anti-GFP at 1:500 (ThermoFisher, A-6455), mouse anti-GFP at 1:300 (ThermoFisher, A-11120), rabbit anti-mCherry at 1:500 (Abcam, ab167453), rabbit anti-Rab7 at 1:2000 (Tanaka and Nakamura, 2008). DAPI was used at 1:1000 (Thermo Fisher Scientific). Secondary antibodies were used at 1:300: goat anti-rabbit (conjugated to Alexa Fluor 647 or Alexa Fluor 568), goat anti-mouse (conjugated to Alexa Fluor 647, Alexa Fluor 488 or Alexa Fluor 568), goat anti-rat (conjugated to Alexa Fluor 647 or Alexa Fluor 568) (ThermoFisher, A-32723, A-11031, A-11036, A-11077, A-32733, A-32728 and A-21247). Discs were equilibrated with Vectashield (Vector Laboratories) for 24-48 h at 4°C before mounting and imaging.

Proximity ligation assay (PLA)

PLA was carried out using Duolink In Situ PLA reagents (Sigma-Aldrich) as described previously (Samarasekera and Auld, 2018) on imaginal wing discs fixed and incubated overnight with the following antibody pairs: rabbit polyclonal (Rb) anti-GFP+mouse monoclonal (mAb) Gli; mAb GFP+Rb anti-Gli; mAb GFP+Rb anti-Scrib; Rb anti-GFP+mAb Dlg. Control PLAs were carried out with Talin endogenously tagged with mCherry plus Gli (Rb anti-mCherry+mAb Gli) or Dlg (Rb anti-mCherry+mAb Dlg). Negative control PLA reactions were carried out with single primary antibodies alone (Rb anti-GFP, or Rb anti-Gli, or mAb Dlg) or no primary antibodies. Samples were equilibrated in

Vectashield (Vector Laboratories) for 2-3 days at 4°C before mounting and imaging.

Imaging

Image stacks were collected with a DeltaVision Spectris microscope (Applied Precision) with a 20× air- or 60× oil-immersion lens (NA1.4) and CoolSnap HQ digital camera. Deconvolution of 0.2 µm *z*-sections with Softworx (Applied Precision) used a point-spread function measured from 0.2-µm beads conjugated with Alexa dyes (Molecular Probes) mounted in Vectashield (Vector Laboratories). Side projections were created using the Softworx program. Images were exported to Photoshop CS (Adobe Systems) for compilation.

Acknowledgements

We would like to thank Drs Bilder, Budnik, Doe, Luschnig and Ward for generous sharing of antibodies and fly lines. The Developmental Studies Hybridoma Bank (DSHB) created by the NICHD of the NIH and maintained at The University of Iowa, Department of Biology, Iowa City, IA 52242 provided monoclonal antibodies used in this study. Stocks obtained from the Bloomington *Drosophila* Stock Center (NIH P40OD018537) were used in this study.

Competing interests

The authors declare no competing or financial interests.

Author contributions

Conceptualization: Z.S., M.M.G., V.J.A.; Methodology: Z.S., M.M.G.; Formal analysis: Z.S., V.J.A.; Investigation: Z.S.; Writing - original draft: Z.S., V.J.A.; Writing - review & editing: Z.S., M.M.G., V.J.A.; Supervision: V.J.A.; Project administration: V.J.A.; Funding acquisition: V.J.A.

Funding

This work was supported by the Canadian Institutes of Health Research [PJT-156320].

Supplementary information

Supplementary information available online at
http://dev.biologists.org/lookup/doi/10.1242/dev.174763.supplemental

References

Albertson, R. and Doe, C. Q. (2003). Dlg, Scrib and Lgl regulate neuroblast cell size and mitotic spindle asymmetry. *Nat. Cell Biol.* **5**, 166-170. doi:10.1038/ncb922

Albertson, R., Chabu, C., Sheehan, A. and Doe, C. Q. (2004). Scribble protein domain mapping reveals a multistep localization mechanism and domains necessary for establishing cortical polarity. *J. Cell Sci.* **117**, 6061-6070. doi:10.1242/jcs.01525

Auld, V. J., Fetter, R. D., Broadie, K. and Goodman, C. S. (1995). Gliotactin, a novel transmembrane protein on peripheral glia, is required to form the blood-nerve barrier in Drosophila. *Cell* **81**, 757-767. doi:10.1016/0092-8674(95)90537-5

Bachmann, A., Draga, M., Grawe, F. and Knust, E. (2008). On the role of the MAGUK proteins encoded by Drosophila varicose during embryonic and postembryonic development. *BMC Dev. Biol.* **8**, 55. doi:10.1186/1471-213X-8-55

Baumgartner, S., Littleton, J. T., Broadie, K., Bhat, M. A., Harbecke, R., Lengyel, J. A., Chiquet-Ehrismann, R., Prokop, A. and Bellen, H. J. (1996). A Drosophila neurexin is required for septate junction and blood-nerve barrier formation and function. *Cell* **87**, 1059-1068. doi:10.1016/S0092-8674(00)81800-0

Bilder, D. (2004). Epithelial polarity and proliferation control: links from the Drosophila neoplastic tumor suppressors. *Genes Dev.* **18**, 1909-1925. doi:10.1101/gad.1211604

Bilder, D. and Perrimon, N. (2000). Localization of apical epithelial determinants by the basolateral PDZ protein Scribble. *Nature* **403**, 676-680. doi:10.1038/35001108

Bilder, D., Li, M. and Perrimon, N. (2000). Cooperative regulation of cell polarity and growth by Drosophila tumor suppressors. *Science* **289**, 113-116. doi:10.1126/science.289.5476.113

Byri, S., Misra, T., Syed, Z. A., Bätz, T., Shah, J., Boril, L., Glashauser, J., Aegerter-Wilmsen, T., Matzat, T., Moussian, B. et al. (2015). The triple-repeat protein anakonda controls epithelial tricellular junction formation in drosophila. *Dev. Cell* **33**, 535-548. doi:10.1016/j.devcel.2015.03.023

Dow, L. E., Kauffman, J. S., Caddy, J., Zarbalis, K., Peterson, A. S., Jane, S. M., Russell, S. M. and Humbert, P. O. (2007). The tumour-suppressor Scribble dictates cell polarity during directed epithelial migration: regulation of Rho GTPase recruitment to the leading edge. *Oncogene* **26**, 2272-2282. doi:10.1038/sj.onc.1210016

Fehon, R. G., Dawson, I. A. and Artavanis-Tsakonas, S. (1994). A Drosophila homologue of membrane-skeleton protein 4.1 is associated with septate junctions and is encoded by the coracle gene. *Development* **120**, 545-557.

Fristrom, D. K. (1982). Septate junctions in imaginal disks of Drosophila: a model for the redistribution of septa during cell rearrangement. *J. Cell Biol.* **94**, 77-87. doi:10.1083/jcb.94.1.77

Genova, J. L. and Fehon, R. G. (2003). Neuroglian, Gliotactin, and the Na+/K+ ATPase are essential for septate junction function in Drosophila. *J. Cell Biol.* **161**, 979-989. doi:10.1083/jcb.200212054

Hall, S., Bone, C., Oshima, K., Zhang, L., McGraw, M., Lucas, B., Fehon, R. G. and Ward, R. E. T. (2014). Macroglobulin complement-related encodes a protein required for septate junction organization and paracellular barrier function in Drosophila. *Development* **141**, 889-898. doi:10.1242/dev.102152

Hildebrandt, A., Pflanz, R., Behr, M., Tarp, T., Riedel, D. and Schuh, R. (2015). Bark beetle controls epithelial morphogenesis by septate junction maturation in Drosophila. *Dev. Biol.* **400**, 237-247. doi:10.1016/j.ydbio.2015.02.008

Hough, C. D., Woods, D. F., Park, S. and Bryant, P. J. (1997). Organizing a functional junctional complex requires specific domains of the Drosophila MAGUK Discs large. *Genes Dev.* **11**, 3242-3253. doi:10.1101/gad.11.23.3242

Humbert, P., Russell, S. and Richardson, H. (2003). Dlg, Scribble and Lgl in cell polarity, cell proliferation and cancer. *BioEssays* **25**, 542-553. doi:10.1002/bies.10286

Ivanov, A. I., Young, C., Den Beste, K., Capaldo, C. T., Humbert, P. O., Brennwald, P., Parkos, C. A. and Nusrat, A. (2010). Tumor suppressor scribble regulates assembly of tight junctions in the intestinal epithelium. *Am. J. Pathol.* **176**, 134-145. doi:10.2353/ajpath.2010.090220

Jacob, L., Opper, M., Metzroth, B., Phannavong, B. and Mechler, B. M. (1987). Structure of the l(2)gl gene of Drosophila and delimitation of its tumor suppressor domain. *Cell* **50**, 215-225. doi:10.1016/0092-8674(87)90217-0

Klapholz, B., Herbert, S. L., Wellmann, J., Johnson, R., Parsons, M. and Brown, N. H. (2015). Alternative mechanisms for talin to mediate integrin function. *Curr. Biol.* **25**, 847-857. doi:10.1016/j.cub.2015.01.043

Mathew, D., Gramates, L. S., Packard, M., Thomas, U., Bilder, D., Perrimon, N., Gorczyca, M. and Budnik, V. (2002). Recruitment of scribble to the synaptic scaffolding complex requires GUK-holder, a novel DLG binding protein. *Curr. Biol.* **12**, 531-539. doi:10.1016/S0960-9822(02)00758-3

McGee, A. W. and Bredt, D. S. (1999). Identification of an intramolecular interaction between the SH3 and guanylate kinase domains of PSD-95. *J. Biol. Chem.* **274**, 17431-17436. doi:10.1074/jbc.274.25.17431

Mendoza, C., Olguin, P., Lafferte, G., Thomas, U., Ebitsch, S., Gundelfinger, E. D., Kukuljan, M. and Sierralta, J. (2003). Novel isoforms of Dlg are fundamental for neuronal development in Drosophila. *J. Neurosci.* **23**, 2093-2101. doi:10.1523/JNEUROSCI.23-06-02093.2003

Morin, X., Daneman, R., Zavortink, M. and Chia, W. (2001). A protein trap strategy to detect GFP-tagged proteins expressed from their endogenous loci in Drosophila. *Proc. Natl. Acad. Sci. USA* **98**, 15050-15055. doi:10.1073/pnas.261408198

Nakajima, Y., Lee, Z. T., McKinney, S. A., Swanson, S. K., Florens, L. and Gibson, M. C. (2019). Junctional tumor suppressors interact with 14-3-3 proteins to control planar spindle alignment. *J. Cell Biol.* **218**, 1824-1838. doi:10.1083/jcb.201803116

Newman, R. A. and Prehoda, K. E. (2009). Intramolecular interactions between the SRC homology 3 guanylate kinase domains of discs large regulate its function in asymmetric cell division. *J. Biol. Chem.* **284**, 12924-12932. doi:10.1074/jbc.M809304200

Nix, S. L., Chishti, A. H., Anderson, J. M. and Walther, Z. (2000). hCASK and hDlg associate in epithelia, and their src homology 3 and guanylate kinase domains participate in both intramolecular and intermolecular interactions. *J. Biol. Chem.* **275**, 41192-41200. doi:10.1074/jbc.M002078200

Noirot-Timothée, C., Graf, F. and Noirot, C. (1982). The specialization of septate junctions in regions of tricellular junctions. II. Pleated septate junctions. *J. Ultrastruct. Res.* **78**, 152-165. doi:10.1016/S0022-5320(82)80020-8

Oda, H., Uemura, T., Harada, Y., Iwai, Y. and Takeichi, M. (1994). A Drosophila homolog of cadherin associated with armadillo and essential for embryonic cell-cell adhesion. *Dev. Biol.* **165**, 716-726. doi:10.1006/dbio.1994.1287

Oshima, K. and Fehon, R. G. (2011). Analysis of protein dynamics within the septate junction reveals a highly stable core protein complex that does not include the basolateral polarity protein Discs large. *J. Cell Sci.* **124**, 2861-2871. doi:10.1242/jcs.087700

Padash-Barmchi, M., Browne, K., Sturgeon, K., Jusiak, B. and Auld, V. J. (2010). Control of Gliotactin localization and levels by tyrosine phosphorylation and endocytosis is necessary for survival of polarized epithelia. *J. Cell Sci.* **123**, 4052-4062. doi:10.1242/jcs.066605

Padash-Barmchi, M., Charish, K., Que, J. and Auld, V. J. (2013). Gliotactin and Discs large are co-regulated to maintain epithelial integrity. *J. Cell Sci.* **126**, 1134-1143. doi:10.1242/jcs.113803

Parnas, D., Haghighi, A. P., Fetter, R. D., Kim, S. W. and Goodman, C. S. (2001). Regulation of postsynaptic structure and protein localization by the Rho-type guanine nucleotide exchange factor dPix. *Neuron* **32**, 415-424. doi:10.1016/S0896-6273(01)00485-8

Paul, S. M., Ternet, M., Salvaterra, P. M. and Beitel, G. J. (2003). The Na+/K+ ATPase is required for septate junction function and epithelial tube-size control in

the Drosophila tracheal system. *Development* **130**, 4963-4974. doi:10.1242/dev.00691

Qian, Y. and Prehoda, K. E. (2006). Interdomain interactions in the tumor suppressor discs large regulate binding to the synaptic protein GukHolder. *J. Biol. Chem.* **281**, 35757-35763. doi:10.1074/jbc.M607057200

Samarasekera, G. D. N. G. and Auld, V. J. (2018). C-terminal Src kinase (Csk) regulates the tricellular junction protein Gliotactin independent of Src. *Mol. Biol. Cell* **29**, 123-136. doi:10.1091/mbc.E17-04-0251

Schneider, C. A., Rasband, W. S. and Eliceiri, K. W. (2012). NIH Image to ImageJ: 25 years of image analysis. *Nat. Methods* **9**, 671-675. doi:10.1038/nmeth.2089

Schulte, J., Tepass, U. and Auld, V. J. (2003). Gliotactin, a novel marker of tricellular junctions, is necessary for septate junction development in Drosophila. *J. Cell Biol.* **161**, 991-1000. doi:10.1083/jcb.200303192

Schulte, J., Charish, K., Que, J., Ravn, S., MacKinnon, C. and Auld, V. J. (2006). Gliotactin and Discs large form a protein complex at the tricellular junction of polarized epithelial cells in Drosophila. *J. Cell Sci.* **119**, 4391-4401. doi:10.1242/jcs.03208

Shin, H., Hsueh, Y.-P., Yang, F.-C., Kim, E. and Sheng, M. (2000). An intramolecular interaction between Src homology 3 domain and guanylate kinase-like domain required for channel clustering by postsynaptic density-95/SAP90. *J. Neurosci.* **20**, 3580-3587. doi:10.1523/JNEUROSCI.20-10-03580.2000

Tanaka, T. and Nakamura, A. (2008). The endocytic pathway acts downstream of Oskar in Drosophila germ plasm assembly. *Development* **135**, 1107-1117. doi:10.1242/dev.017293

Tejedor, F. J., Bokhari, A., Rogero, O., Gorczyca, M., Kim, E., Sheng, M., Bhandari, P., Singh, S. and Budnik, V. (1997). Essential role for dlg in synaptic clustering of Shaker K^+ Channels in vivo. *J. Neurosci.* **17**, 152-159. doi:10.1523/JNEUROSCI.17-01-00152.1997

Tepass, U. and Hartenstein, V. (1994). The development of cellular junctions in the Drosophila embryo. *Dev. Biol.* **161**, 563-596. doi:10.1006/dbio.1994.1054

Tsukita, S., Furuse, M. and Itoh, M. (2001). Multifunctional strands in tight junctions. *Nat. Rev. Mol. Cell Biol.* **2**, 285-293. doi:10.1038/35067088

Venema, D. R., Zeev-Ben-Mordehai, T. and Auld, V. J. (2004). Transient apical polarization of Gliotactin and Coracle is required for parallel alignment of wing hairs in Drosophila. *Dev. Biol.* **275**, 301-314. doi:10.1016/j.ydbio.2004.07.040

Venken, K. J. T., Schulze, K. L., Haelterman, N. A., Pan, H., He, Y., Evans-Holm, M., Carlson, J. W., Levis, R. W., Spradling, A. C., Hoskins, R. A. et al. (2011). MiMIC: a highly versatile transposon insertion resource for engineering Drosophila melanogaster genes. *Nat. Methods* **8**, 737-743. doi:10.1038/nmeth.1662

Voelker, R. A., Wisely, G. B., Huang, S. and Gyurkovics, H. (1985). Genetic and molecular variation in the RpII215 region of Drosophilia melanogaster. *Mol. Gen. Genet.* **201**, 437-445. doi:10.1007/bf00331336

Wang, S., Yoo, S., Kim, H.-Y., Wang, M., Zheng, C., Parkhouse, W., Krieger, C. and Harden, N. (2015). Detection of in situ protein-protein complexes at the Drosophila larval neuromuscular junction using proximity ligation assay. *J. Vis. Exp.* e52139. doi:10.3791/52139

Woods, D. F. and Bryant, P. J. (1991). The discs-large tumor suppressor gene of Drosophila encodes a guanylate kinase homolog localized at septate junctions. *Cell* **66**, 451-464. doi:10.1016/0092-8674(81)90009-X

Woods, D. F., Hough, C., Peel, D., Callaini, G. and Bryant, P. J. (1996). Dlg protein is required for junction structure, cell polarity, and proliferation control in Drosophila epithelia. *J. Cell Biol.* **134**, 1469-1482. doi:10.1083/jcb.134.6.1469

Zeitler, J., Hsu, C. P., Dionne, H. and Bilder, D. (2004). Domains controlling cell polarity and proliferation in the Drosophila tumor suppressor Scribble. *J. Cell Biol.* **167**, 1137-1146. doi:10.1083/jcb.200407158

Figure S1

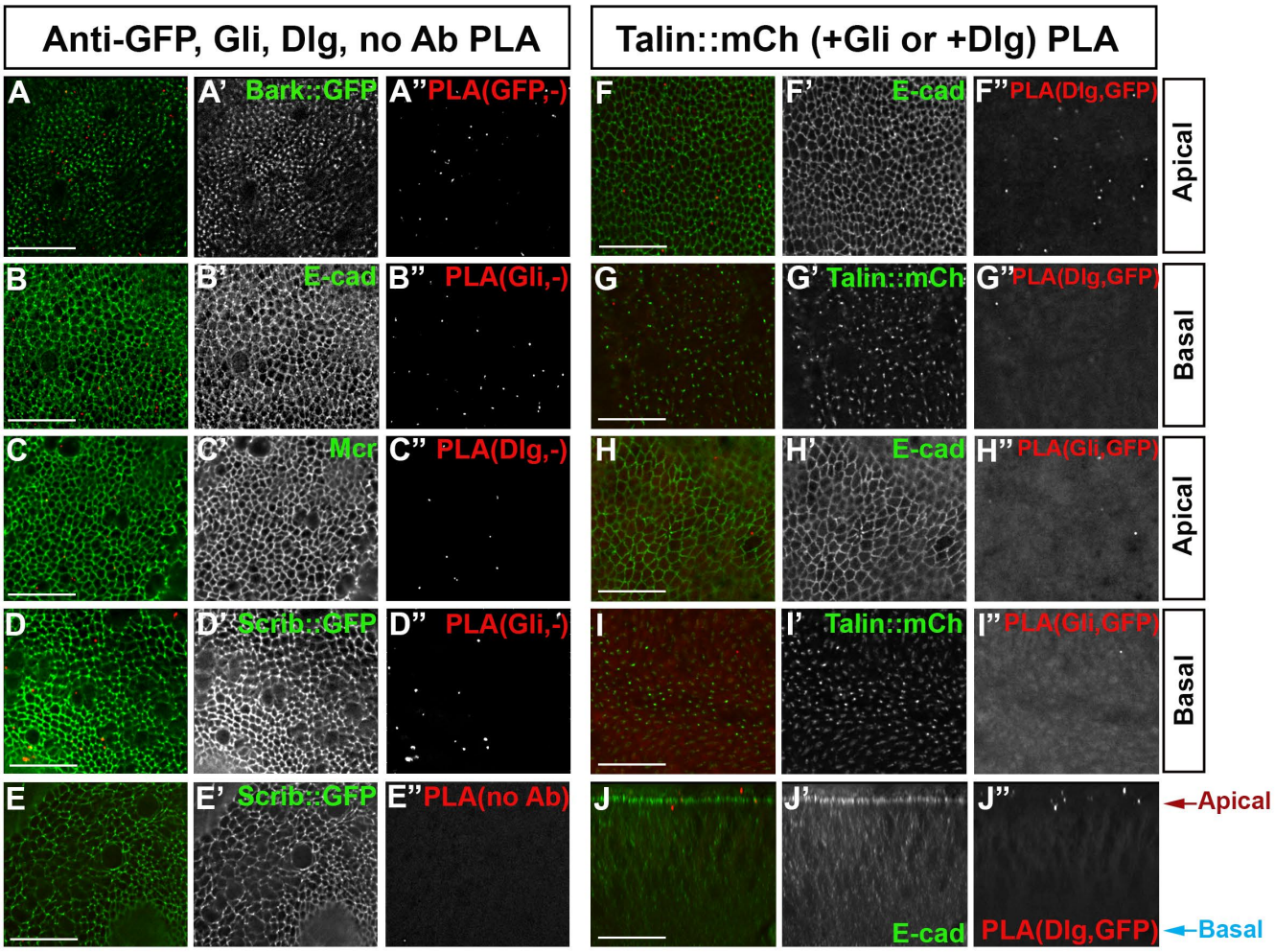

Figure S1: Controls for PLA assays

(A-E) PLA reactions were carried out using either a single antibody or no antibody as PLA controls in wing disc columnar epithelia.

(A) Bark::GFP (green, A') wing disk with PLA reaction using only anti-GFP (red, A").

(B) PLA using only the anti-Gli antibody (red, B"), and with E-cad immunolabeling (green, B').

(C) PLA using only the anti-Dlg antibody (red, C"), and with Mcr immunolabeling (green, C').

(D) Scrib::GFP (green, D') wing disk with PLA using only the anti-Gli antibody (red, D").

(E) Scrib::GFP (green, E') wing disk and PLA with no primary antibodies (red, E").

(F-J) Negative control with testing PLA between Talin tagged with mCherry (Talin::mCherry) +Gli or +Dlg in wing disc columnar epithelia using the mCherry antibody and Dlg or Gli antibodies.

(F-G) PLA between Talin::mCh+Dlg. (F) An apical z-slice immunolabeled for E-cad (green, F') showing the lack of PLA between Dlg and Talin::mCh (red, F''). (G) A basal z-slice showing Talin::mCh focal adhesions (green, G') showing the lack of PLA between Dlg and Talin::mCh (red, G'').

(H-I) PLA between Talin::mCh+Gli. (H) An apical z-slice with E-cad immunolabeling (green, H') showing the lack of PLA between Gli and Talin::mCh (red, H''). (I) Basal z-slice with Talin::mCh focal adhesions (green, I') showing the lack of PLA between Gli and Talin::mCh (red, I'').

(J) A side projection showing apical Ecad immunolabeling (green, J') and the lack of PLA between Dlg and Talin::mCh (red, J'').

All en-face panels represent a single z slice. Scale bars: 15 μm.

Figure S2

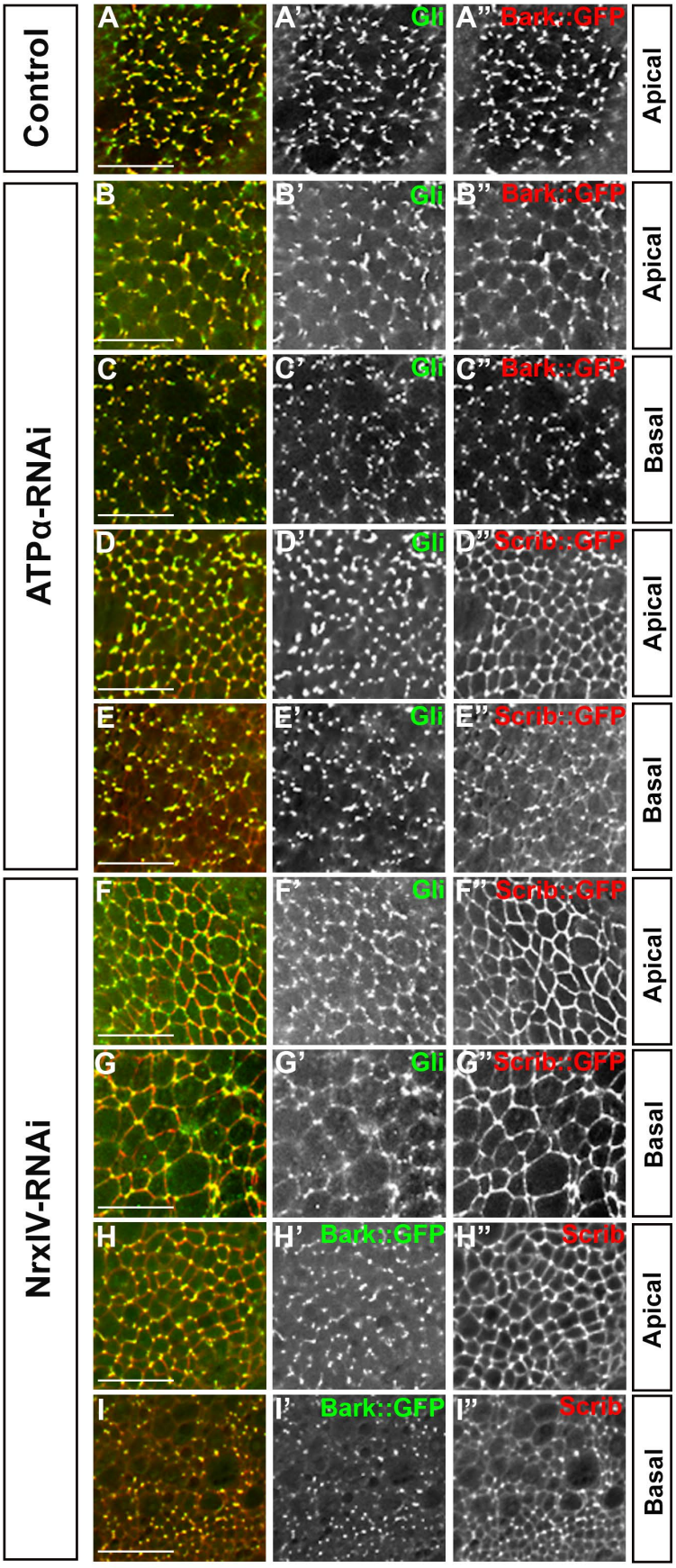

Figure S2: Tricellular expression of Gli, Bark, and Scrib is retained in SJ protein knockdown

(A) The normal expression of Gli (green, A') and Bark::GFP (red, A") is shown at the TCJ in the columnar epithelia. (B-I) apterous-GAL4 was used to drive expression of ATPα-RNAi or NrxIV-RNAi in the dorsal side of the wing disc. All panels show 2X digital magnifications of the apterous side of the wing disc from Fig. 5A-L. (B-E) ATPα-RNAi mediated knockdown led to the basolateral spread of Gli (green, B'-E'), Bark (red, B", C") and Scrib (red, D", E"). Gli (green, B', D'), Bark (red, B") and Scrib (red, D") were concentrated to the TCJ at the level of the SJ domain and still retained in the TCJ in more basal regions (C, E). (F-I) NrxIV knockdown through NrxIV-RNAi led the basolateral spread of Gli (green, F', G'), Scrib (red, F"-I"), and Bark (red, H', I'). Gli (green, G'), Scrib (red, G", I") and Bark (I') were concentrated to the corner of the cells in the basal side. All xy panels represent a single z slice. Scale bars: 15 μm.